DEPDC1B promotes migration and invasion in pancreatic ductal adenocarcinoma by activating the Akt/GSK3β/Snail pathway

XU LIU[*], TONG LI[*], XINYANG HUANG, WEI WU, JUANJUAN LI, LUMIN WEI, YUTING QIAN, HUI XU, QI WANG and LIFU WANG

Department of Gastroenterology, Ruijin Hospital Affiliated with Shanghai Jiao Tong University School of Medicine, Shanghai 200025, P.R. China

Abstract. Pancreatic ductal adenocarcinoma (PDAC) is a highly lethal disease, which frequently presents with distant metastasis. Further understanding of the molecular mechanism of PDAC is helpful to uncover novel and effective therapeutic strategies. DEP domain containing 1B (DEPDC1B) is known to play a role in the carcinogenesis and metastasis of several common types of cancer; however, its biological function and molecular mechanism in PDAC progression remain unclear. In the present study, the expression levels of DEPDC1B were detected in 79 pairs of PDAC and adjacent non-cancerous tissues. Patients with PDAC that exhibited higher DEPDC1B expression levels, were shown to have a poorer prognosis. Functional studies showed that knocking down DEPDC1B inhibited PDAC cell migration and invasion, while over-expressing DEPDC1B promoted these processes. Western blotting analysis and immunofluorescence demonstrated that DEPDC1B overexpression induced the epithelial-to-mesenchymal transition (EMT). Further mechanistic studies revealed that DEPDC1B was able to activate the Akt/glycogen synthase kinase-3β (GSK3β)/Snail signaling pathway. In conclusion, the results of the present study showed that DEPDC1B may serve as an oncogene that contributes to PDAC cell migration and invasion by inducing EMT via Akt/GSK3β/Snail pathway activation.

Correspondence to: Professor Lifu Wang or Dr Qi Wang, Department of Gastroenterology, Ruijin Hospital Affiliated with Shanghai Jiao Tong University School of Medicine, 197 Ruijin Er Road, Shanghai 200025, P.R. China
E-mail: lifuwang@sjtu.edu.cn
E-mail: wangqilaile@hotmail.com

[*]Contributed equally

Introduction

Pancreatic ductal adenocarcinoma (PDAC) is the most lethal gastrointestinal malignancy with close parallels between incidence and mortality (1,2). In China, ~90,100 new cases of PDAC and 79,400 PDAC-associated mortality cases were estimated in 2015 (3). Although advancements have been made in PDAC treatment, the prognosis of patients with PDAC remains poor, primarily due to the frequency of distant metastasis. Therefore, it is still urgent to investigate the molecular mechanisms underlying PDAC progression and identify novel therapeutic strategies to improve the outcome of patients with PDAC.

The DEP domain containing 1B (DEPDC1B) gene is located at the human chromosome 5q12.1, and encodes a protein containing a Dishevelled, EGL-10 and pleckstrin (DEP) domain and a Rho-GTPase-activating protein-like domain. The precise function of DEPDC1B has not yet been clarified, but studies have shown its association with a variety of cell events, including cell proliferation, cell adhesion and cell cycle regulation (4-6). In addition, previous studies have also claimed that DEPDC1B has an oncogenic effect in breast carcinoma, non-small cell lung cancer (NSCLC), prostate cancer, malignant melanoma and oral cancer (7-11). However, the biological function of DEPDC1B in PDAC has not yet been investigated.

Tumor metastasis is the leading cause of cancer-associated mortality (12). It is well known that epithelial-to-mesenchymal transition (EMT) plays a crucial role in the initiation and promotion of cancer cell invasion and dissemination (13-15). Cancer cells that have undergone EMT lose their epithelial characteristics and obtain the ability to invade other tissues (16). Loss of E-cadherin is regarded as a key event of EMT (17). At the same time, during EMT, the expression levels of mesenchymal markers such as N-cadherin and Vimentin are often upregulated (18). Previous studies have reported that EMT is involved in the dissemination of cancer cells in PDAC (18-20). It has also been reported that the Akt/glycogen synthase kinase-3β (GSK3β)/Snail signaling pathway regulates EMT and metastasis (21-23). Activation of Akt can enhance Snail nucleus accumulation by facilitating GSK3β degradation, subsequently inducing EMT and cancer metastasis (24-26).

In the present study, the role of DEPDC1B in PDAC and the association between DEPDC1B expression in PDAC tissues and patient prognosis was analyzed. DEPDC1B silencing was found to inhibit PDAC cell proliferation, migration and invasion, whereas DEPDC1B overexpression exerted the opposite effect. Results also suggested that DEPDC1B activated the Akt/GSK3β/Snail signaling pathway and triggered EMT. Collectively, the present findings suggested that DEPDC1B may be an important regulator of PDAC progression and a potential target for future PDAC treatment.

Materials and methods

Gene Expression Omnibus (GEO) data analysis. A total of three PDAC datasets [GSE15471 (27), GSE16515 (28) and GSE32676 (29)] were obtained from the GEO database (https://www.ncbi.nlm.nih.gov/geo/). The raw probe-level data (CEL files) and annotations for the probe arrays downloaded from GEO were used for analysis conducted by R software (version 3.5.0). The robust multi-array average algorithm in the Affy package of R was used for data pre-processing including background correction and quantile normalization. Then the probe ID was transformed to gene symbols. For multiple probe sets corresponding to the same gene, their average expression value was taken as the gene expression value.

Patients and tissue samples. A total of 79 pairs of PDAC tissues and adjacent non-cancerous tissues were collected from patients who underwent surgical resection at Ruijin Hospital Affiliated with Shanghai Jiao Tong University School of Medicine (Shanghai, China) between January 2011 and December 2017. All patients were diagnosed with PDAC via pathological diagnosis and had not received chemotherapy or radiotherapy before resection. The present study was approved by the Ethics Committee of Ruijin Hospital, and informed consent was obtained from all patients included in the study.

Cell culture and reagents. The human pancreatic cancer cell lines BxPC-3, MIA PaCa-2, PANC-1 and SW1990 were purchased from the Cell Bank of the Chinese Academy of Sciences. Capan-1, Capan-2 and the normal human pancreatic ductal cell line hTERT-HPNE were purchased from the American Type Culture Collection. Cells were cultured in Dulbecco's modified Eagle's medium (DMEM; Gibco; Thermo Fisher Scientific, Inc.) containing 10% fetal bovine serum (FBS; Lonsera Science) and 1% penicillin/streptomycin at 37°C with 5% CO_2. LY294002 was purchased from Absin (cat. no. abs810001).

Immunohistochemistry (IHC) and tissue microarray (TMA). A TMA including 79 pairs of matched PDAC tissues and adjacent non-cancerous tissues was analyzed. The immunohistochemical procedure was described in our previous study (30). An antibody against DEPDC1B (1:100; cat. no. PA5-72875; Invitrogen; Thermo Fisher Scientific, Inc.) was used to detect the protein expression levels according to the standard procedure (30). The final IHC score was calculated by multiplying the percentage of positive cells (0, ≤5%; 1, 5-25%; 2, 25-50%; 3, 50-75%; 4, >75%) by the intensity scores (0, negatively stained; 1, weakly stained; 2, moderately stained; 3, strongly stained). Patients with a score ≥4 were regarded as having high expression of DEPDC1B. In contrast, patients with an IHC score <4 were described as having low expression.

RNA extraction and reverse transcription quantitative PCR (RT-qPCR). Total RNA of hTERT-HPNE and pancreatic cancer cells was extracted using TRIzol® reagent (Invitrogen; Thermo Fisher Scientific, Inc.). A total of 2 μg of total RNA was used to synthesize cDNA with the First Strand cDNA Synthesis SuperMix for RT-qPCR (Shanghai Yeasen Biotechnology Co., Ltd.), according to the manufacturer's protocol. Then, qPCR reactions were performed using SYBR Green Master Mix (Shanghai Yeasen Biotechnology Co., Ltd.) on a StepOnePlus Real-Time PCR system (Applied Biosystems; Thermo Fisher Scientific, Inc.), according to the manufacturer's instructions. Relative mRNA expression was analyzed using the $2^{-\Delta\Delta Cq}$ method and normalized to GAPDH (31). RT was performed at 42°C for 15 min, followed by 2 min at 85°C. The qPCR program used included an initial denaturation at 90°C for 5 min, followed by 40 cycles of denaturation at 90°C for 10 sec and annealing/elongation at 60°C for 30 sec. The primers used were as follows: DEPDC1B: Forward, 5'-CCACCAGGC ACTTCACAAGAGAAC-3'; and reverse, 5'-CGGTGGACA AGACGGCAAGC-3'; GAPDH: Forward, 5'-CAGGAGGCA TTGCTGATGAT-3'; and reverse, 5'-GAAGGCTGGGGC TCATTT-3'.

Western blot analysis. Total protein was isolated from hTERT-HPNE and pancreatic cancer cells using RIPA containing 1% PMSF (both from Beyotime Institute of Biotechnology) according to the manufacturer's protocol. Protein concentrations were determined using the BCA Protein Assay kit (Beyotime Institute of Biotechnology). Protein samples (30-60 μg per lane) were separated with 10% SDS-PAGE gels and transferred to PVDF membranes (EMD Millipore). Then, the membranes were blocked in TBS-Tween-20 containing 5% fat-free milk for 2 h at room temperature and incubated with the primary antibodies overnight at 4°C with gentle shaking. The primary antibodies included DEPDC1B (1:1,000; cat. no. PA5-72875; Invitrogen; Thermo Fisher Scientific, Inc.), E-cadherin (1:1,000; cat. no. 3195T), N-cadherin (1:1,000; cat. no. 131116T), Vimentin (1:1,000; cat. no. 3932S), Snail (1:1,000; cat. no. 3879S), Slug (1:1,000; cat. no. 9585T), Akt (1:1,000; cat. no. 4691S), and phosphorylated (p)-GSK-3β (1:1,000; cat. no. 5558S) (all from Cell Signaling Technology, Inc.), Twist (1:1,000; cat. no. ab49254; Abcam), p-Akt-S473 (1:1,000; cat. no. AP0140; ABclonal Biotech Co., Ltd.), GSK-3β (1:1,000; cat. no. A16868; ABclonal Biotech Co., Ltd.), and GAPDH (1:2,000, cat. no. GB12002, Servicebio; Stratech). After washing with TBST three times, the membranes were incubated with the corresponding horseradish peroxidase-conjugated secondary antibodies (1:5,000; cat. no. 7074P2 and 7076S; Cell Signaling Technology, Inc.) at room temperature for 1 h. Signals were detected using enhanced chemiluminescence regent (GE Healthcare Bio-Sciences).

Lentivirus-mediated interference or overexpression. Validated small interfering (si)RNA targeting human DEPDC1B (5'-TGCTAGATTGGTAACGTTT-3') and its corresponding

negative control (NC; 5'-TTCTCCGAACGTGTCACGT-3') were synthesized and inserted into the lentiviral vector GV248 by GeneChem, Inc. For DEPDC1B overexpression, the coding sequence (CDS) of DEPDC1B was amplified and cloned into pHBLV-CMV-MCS-3FLAG-EF1-ZsGreen-T2A-PURO vector. The empty vector was used as the negative control for the overexpression assay. Recombinant lentiviruses overexpressing DEPDC1B and the negative control were provided by Hanbio Biotechnology Co., Ltd.

For the inhibition and overexpression of DEPDC1B, PDAC cells (Capan-1, SW1990, MIA PaCa-2 and PANC-1) were cultured to 30-50% confluence and transfected with lentivirus and polybrene overnight at the MOI (multiplicity of infection) of 10-30 according to the manufacturer's protocol. Stable transfected cells were selected in culture medium containing puromycin ($2\ \mu g/ml$) for 10 days.

Cell Counting Kit-8 (CCK-8) assay. To measure cell viability, the transfected pancreatic cancer cells were seeded in 96-well plates ($1x10^3$ cells/well). A total of 100 μl complete culture medium containing 10 μl CCK-8 reagent (Beyotime Institute of Biotechnology) was added to each well at different time points of interest. After incubation in the dark at 37°C for 2 h, the absorption at 450 nm was detected. Each group had five duplicate wells and the experiments were repeated in triplicate.

Colony formation assay. Different cells were plated in 6-well plates (500 cells/well) in triplicate. Cells were maintained in culture for 14 days, and were then fixed with 4% paraformaldehyde (Beyotime Institute of Biotechnology) at room temperature for 20 min followed by staining with crystal violet solution (Beyotime Institute of Biotechnology) at room temperature for 30 min. Images were captured with a camera and the colonies were counted manually to access cell proliferation ability.

Wound healing assay. Capan-1, SW1990, MIA PaCa-2 and PANC-1 cells were seeded into 6-well plates at a density of $5x10^5$/well and maintained in culture until 100% confluent. At that point, wounds were made using a standard 200 μl pipette tip. Cells were washed with PBS to remove debris and cultured in DMEM without FBS. Images were captured at 0 and 48 h after scratching with a light microscope (magnification, x200; Nikon Corporation). The cell migratory ability was evaluated by measuring the percentage of wound healing. The 48 h wound healing percentage=(0 h area of wound-48 h area of wound)/(0 h area of wound).

Transwell assay. Transwell chambers (Corning, Inc.) precoated with or without Matrigel (BD Biosciences) for 30 min at 37°C were used for invasion and migration assays, respectively. A total of 600 μl of DMEM containing 10% FBS was added to the lower chambers, and $5x10^4$ cells suspended in 200 μl of serum-free DMEM were placed in the upper chambers. After 24 h in culture, migrated and invaded cells were fixed with 4% paraformaldehyde and stained with crystal violet staining solution at room temperature for 10 min. Cells in the lower chamber were removed using a cotton-tipped swab. Finally, the numbers of migrated and invaded cells in five randomly selected fields were counted under a light microscope (magnification, x200; Nikon Corporation).

Immunofluorescence. Cells were seeded on glass coverslips and maintained in culture for 24 h. Then cells were fixed with 4% paraformaldehyde at room temperature for 15 min, permeabilized with 0.3% Triton X-100 at room temperature for 10 min and blocked with 0.3% BSA (Shanghai Yeasen Biotechnology Co., Ltd.) in PBS at room temperature for 30 min. Then, primary antibodies against E-cadherin (1:50; cat. no. 20874-1-AP), N-cadherin (1:100; cat. no. 66219-1-Ig) (both from Proteintech Group, Inc.) and Vimentin (1:100; cat. no. 3932S; Cell Signaling Technology, Inc.) were added and incubated overnight in a humidified chamber at 4°C. On the following day, Alexa Fluor 555-labeled Donkey Anti-Rabbit IgG (H+L) (1:200; cat. no. A0453; Beyotime Institute of Biotechnology) or IFKine™ Red Donkey Anti-Mouse IgG (1:200; cat. no. A24411; Abbkine Scientific Co., Ltd.) were applied and incubated for 1 h in the dark at room temperature. Finally, the nuclei of cells were counterstained with DAPI (Servicebio; Stratech) at room temperature for 5 min. All washes were performed with PBS. Images were captured with a fluorescence microscope (magnification, x400; Nikon Corporation).

Xenograft tumor study. A total of 10 female BALB/c nude mice (age, 4-5 weeks; body weight, 12-16 g) were purchased from the Shanghai Experimental Animal Center of the Chinese Academy of Sciences and housed (5 mice per cage) under standard conditions (26°C, 40-60% relative humidity, 12 h light/dark cycles) with unlimited access to food and water. Animal health and behavior were monitored every day. For tumor metastasis assays, DEPDC1B knockdown and negative control Capan-1 cells ($3x10^6$ cells) were intravenously injected into the tail vein of female 6-week-old nude mice (n=5 per group). After 10 weeks, the mice were euthanized in a gradually filled CO_2 chamber with a flow rate of ≤30% CO_2 of the chamber volume/min. The death was verified by the absence of respiratory movement and heartbeat. The lungs of the mice were dissected for H&E staining to assess the lung metastatic foci. All animal experiments were approved by the Institutional Animal Care and Use Committee of Shanghai Jiaotong University School of Medicine (IACUC approval no. B-2019-004).

Statistical analysis. All data were analyzed using SPSS software (version 20.0; IBM Corp.) and are presented as the mean ± standard error (n≥3). Student's t-test was used to assess the statistical significance between two groups. One-way ANOVA followed by the Least Significant Difference post hoc test was used to compare multiple groups. The χ^2 test was used to analyze the association between DEPDC1B expression and clinicopathological parameters. Survival analysis was evaluated using the Kaplan-Meier method and log-rank test. $P<0.05$ was considered to indicate a statistically significant difference.

Results

Upregulation of DEPDC1B in tumor tissues is associated with poor prognosis in patients with PDAC. The three datasets (GSE15471, GSE16515 and GSE32676) were analyzed from the GEO database and the results showed that DEPDC1B mRNA was significantly upregulated in PDAC tissues compared with
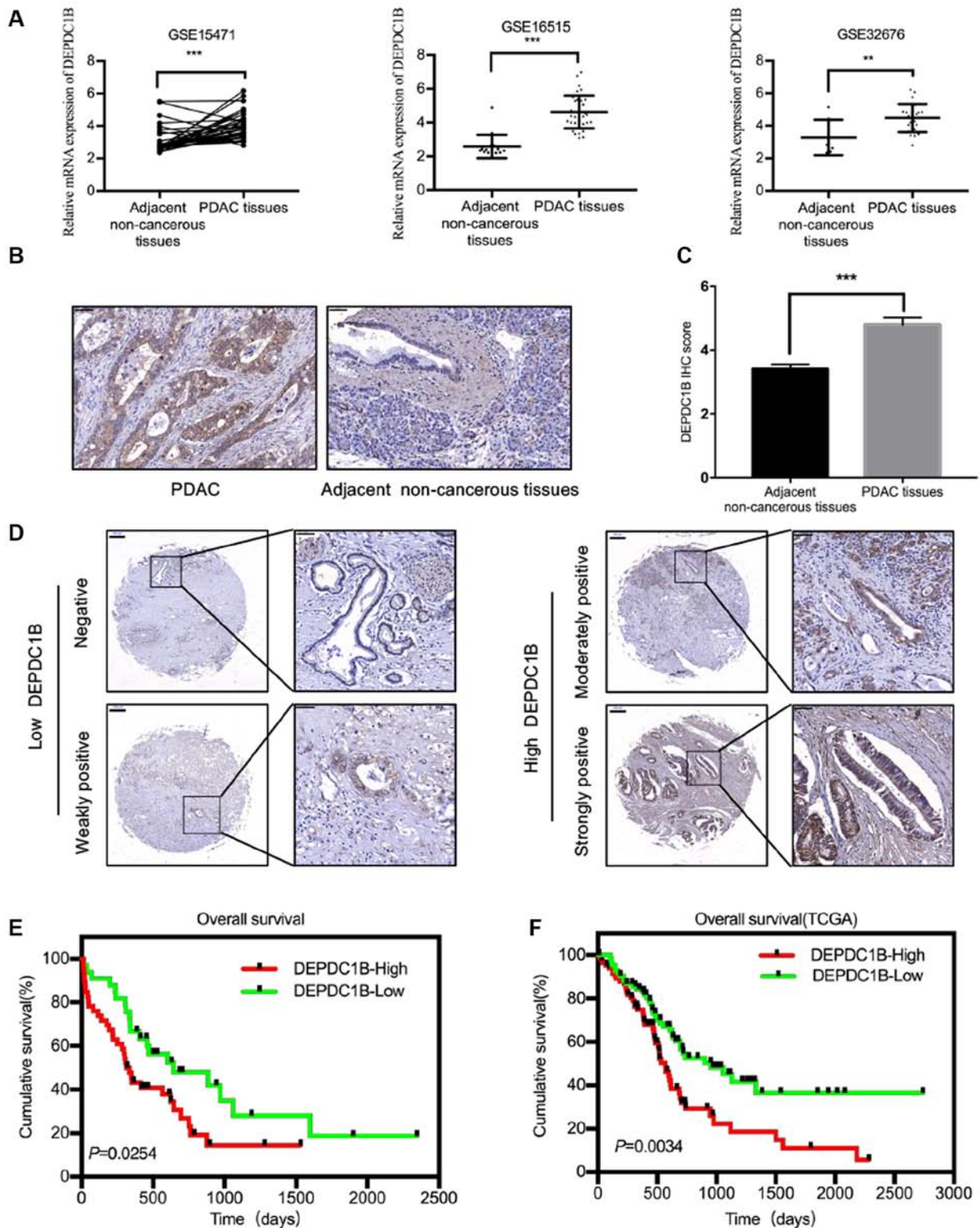
Figure 1. DEPDC1B expression is increased in PDAC tissues. (A) The GEO datasets (GSE15471, GSE16515 and GSE32676) showed that the DEPDC1B mRNA expression levels were upregulated in PDAC tissues. (B) Representative IHC staining images for DEPDC1B in PDAC and adjacent non-cancerous tissues. Scale bar, 50 μm. (C) DEPDC1B IHC score in PDAC tissues and adjacent non-cancerous tissues on TMAs. (D) Representative IHC staining images for DEPDC1B expression levels in TMAs. Scale bar, 200 μm (left), 50 μm (right). (E and F) Kaplan-Meier analysis showed the association between DEPDC1B expression and patient prognosis. **P<0.01; ***P<0.001. DEPDC1B, DEP domain containing 1B; GEO, Gene Expression Omnibus; PDAC, pancreatic ductal adenocarcinoma; IHC, immunohistochemistry; TCGA, The Cancer Genome Atlas; TMAs, tissue microarrays.

that in adjacent non-cancerous tissues (Fig. 1A). To further confirm this finding, immunohistochemical analysis were performed in a TMA containing 79 samples of PDAC and

adjacent non-cancerous tissues (Fig. 1B). According to the IHC score, the expression levels of DEPDC1B were higher in PDAC tissues than those in paired non-cancerous tissues

Table I. Associations between DEPDC1B low expression (n=32) and DEPDC1B high expression (n=47) and clinicopathologic characteristics of patients with pancreatic ductal adenocarcinoma.

Clinicopathological characteristics	Total (n=79)	DEPDC1B level		P-value
		Low, n	High, n	
Sex				0.156
Female	32	16	16	
Male	47	16	31	
Age, years				0.107
<60	17	4	13	
≥60	62	28	34	
Tumor size, cm				0.094
<5	56	26	30	
≥5	23	6	17	
Primary tumor(T)				0.352
T1+T2	52	23	29	
T3+T4	27	9	18	
Lymph node metastasis				0.957
Absent	59	24	35	
Present	20	8	12	
Metastasis				0.391
No	76	32	44	
Yes	3	0	3	
TNM [AJCC (44)]				0.464
I+II	38	17	21	
III+IV	41	15	26	
Nerve invasion				0.143
Absent	35	11	24	
Present	44	21	23	

DEPDC1B, DEP domain containing 1B; TNM, Tumor-Node-Metastasis; AJCC, American Joint Committee on Cancer.

(Fig. 1C and D). No significant association between DEPDC1B expression levels and the clinicopathological characteristics of the samples was observed (Table I). However, Kaplan-Meier survival analysis revealed that patients with PDAC with higher expression levels of DEPDC1B could have a shorter survival time (Fig. 1E). Meanwhile, the data from The Cancer Genome Atlas also verified the association between high DEPDC1B expression and poor prognosis (Fig. 1F).

DEPDC1B expression in PDAC cell lines and construction of a stable cell line. DEPDC1B expression was detected in six PDAC cell lines and the normal pancreatic cells hTERT-HPNE by RT-qPCR and western blotting. Higher expression of DEPDC1B was observed in PDAC cell lines compared with hTERT-HPNE (Fig. 2A and C). Capan-1 and SW1990 cells with high DEPDC1B expression, MIA PaCa-2 and PANC-1 cells with low DEPDC1B expression were selected for following experiments. Through a lentiviral delivery system, DEPDC1B was stably knocked down in Capan-1 and SW1990 cells and overexpressed in MIA PaCa-2 and PANC-1 cells. The transfection efficiency was confirmed by RT-qPCR and western blotting (Fig. 2B and D).

DEPDC1B promotes the proliferation, migration and invasion of PDAC cells. Considering the association between high DEPDC1B expression and poor prognosis, the role of DEPDC1B in cell proliferation, migration and invasion was further investigated. CCK-8 assay and colony formation assays revealed that cell proliferation was inhibited by DEPDC1B knockdown and promoted by DEPDC1B overexpression (Fig. 2E and F). Wound healing and Transwell assays were performed to investigate the role of DEPDC1B in cell migration and invasion. The wound healing assay showed that silencing DEPDC1B inhibited the migratory ability of Capan-1 and SW1990 cell lines, whereas DEPDC1B overexpression increased the wound healing rate of MIA PaCa-2 and PANC-1 cells (Fig. 3A). Transwell assays indicated that knockdown of DEPDC1B suppressed the migration and invasion of PDAC cells, while DEPDC1B overexpression promoted PDAC cell migration and invasion (Fig. 3B).
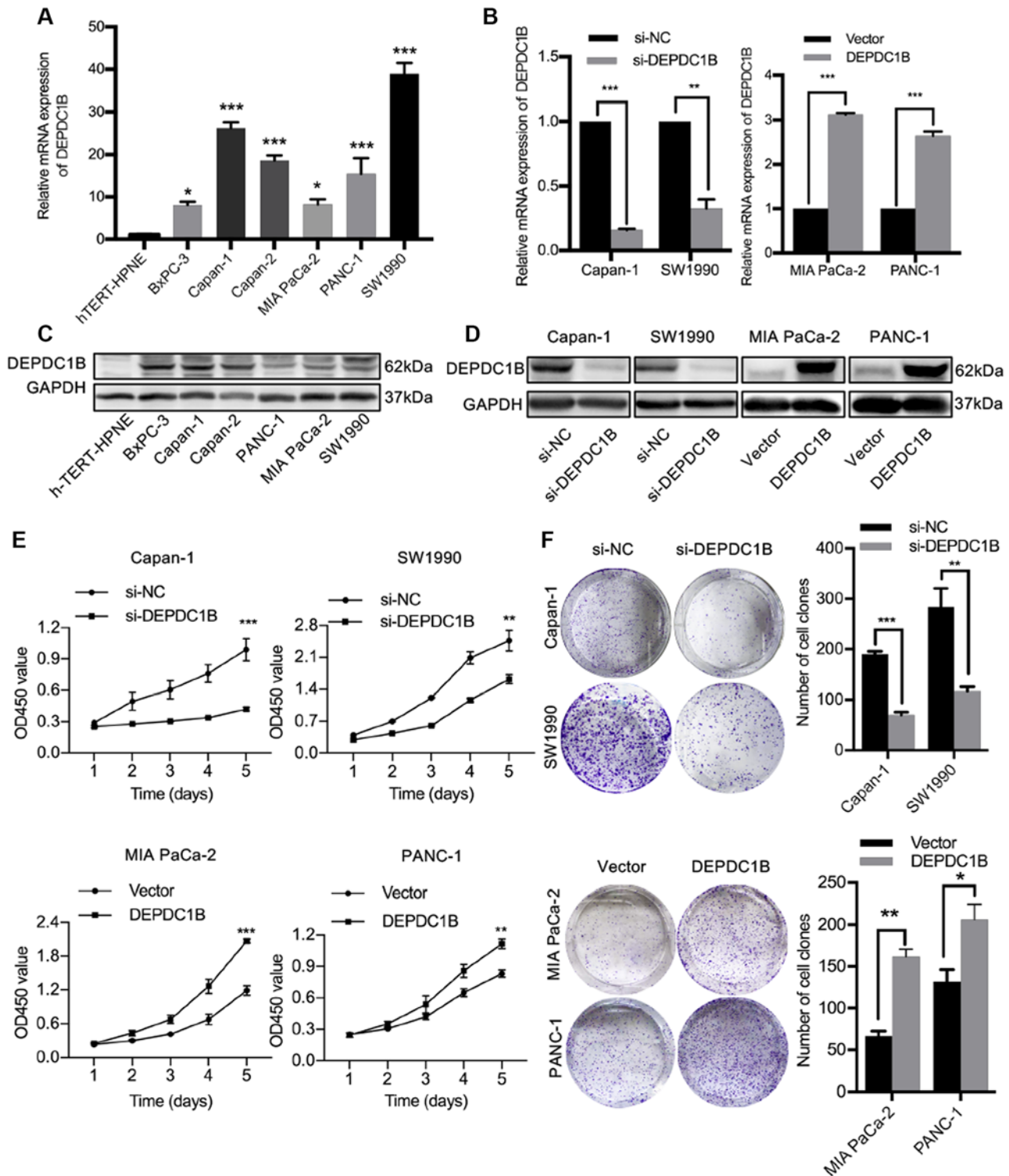
Figure 2. DEPDC1B expression in PDAC cell lines and the effect of DEPDC1B on PDAC cell proliferation. (A) The DEPDC1B mRNA expression levels were detected in PDAC cell lines and compared with normal pancreatic cells hTERT-HPNE. (B) The DEPDC1B knockdown and overexpression efficiencies were measured by reverse transcription-quantitative PCR. (C) The DEPDC1B protein expression levels were detected in hTERT-HPNE and several PDAC cell lines by western blotting. (D) The DEPDC1B knockdown and overexpression efficiencies were measured by western blotting. (E) Cell Counting Kit-8 assays demonstrated that DEPDC1B knockdown suppressed PDAC cell proliferation, whereas the overexpression of DEPDC1B promoted PDAC cell proliferation. (F) DEPDC1B knockdown inhibited colony formation of PDAC cells, but the overexpression of DEPDC1B increased colony formation. *P<0.05; **P<0.01; ***P<0.001. NC, negative control; si, small interfering RNA; DEPDC1B, DEP domain containing 1B; PDAC, pancreatic ductal adenocarcinoma.

To further investigate the effect of DEPDC1B on tumor metastasis *in vivo*, a lung metastatic model was established in nude mice. The results demonstrated that the incidence of lung metastasis in the si-DEPDC1B group was lower than that in the control group (Fig. 4). The mean tumor diameter in the control group was 1.0 mm and the largest tumor measured 6.0 mm. No metastatic nodules were observed in the si-DEPDC1B group.
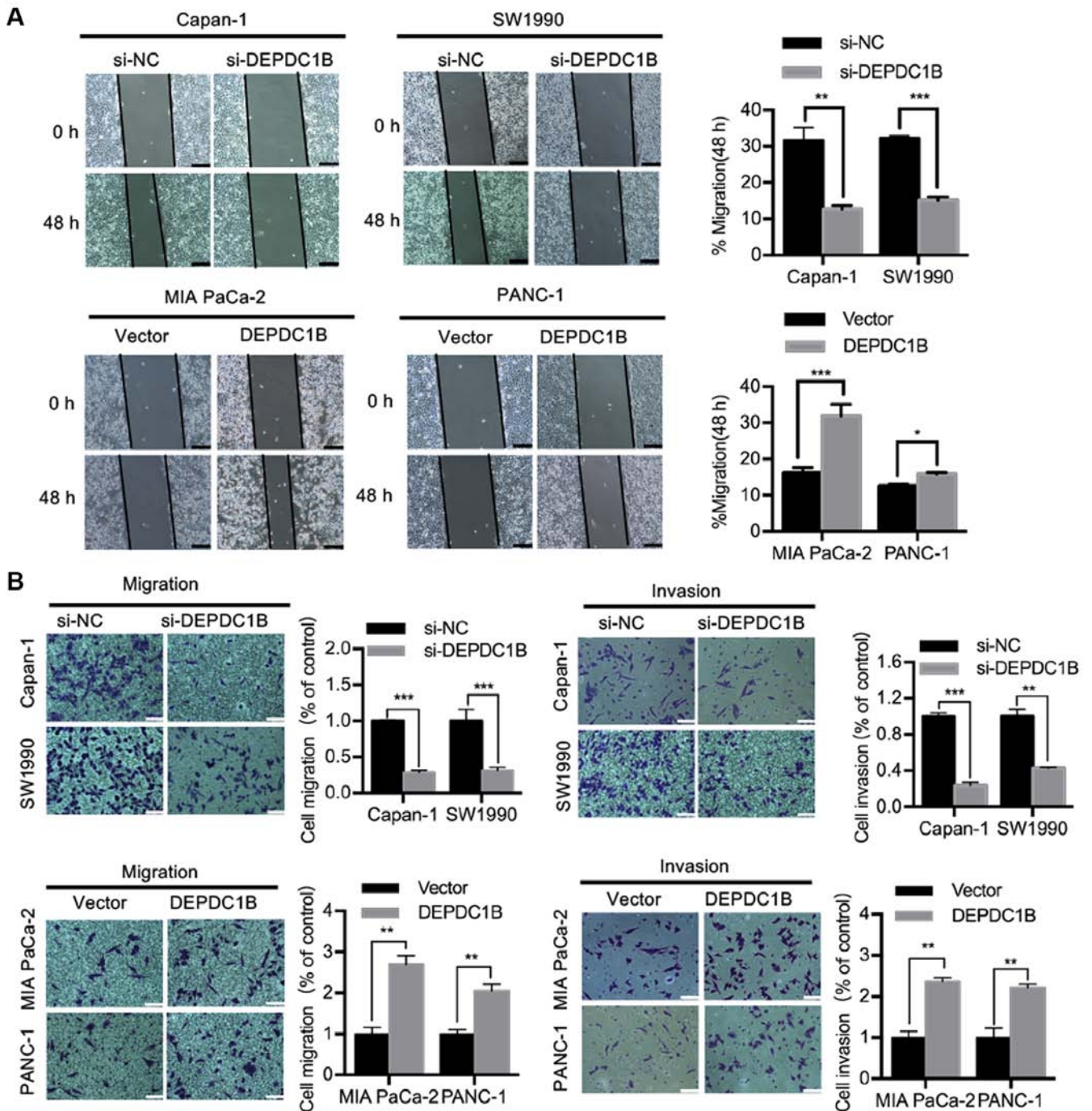
Figure 3. DEPDC1B promotes PDAC cell migration and invasion. (A) Wound healing assays displayed the effect of DEPDC1B on PDAC cell migration. Scale bar, 100 μm. (B) Transwell assays showed the effect of DEPDC1B on cell migration and invasion. Scale bar, 100 μm. *P<0.05; **P<0.01; ***P<0.001. NC, negative control; si, small interfering RNA; DEPDC1B, DEP domain containing 1B; PDAC, pancreatic ductal adenocarcinoma.

DEPDC1B regulates EMT in PDAC cells. EMT is an important event in tumor metastasis, which allows cancer cells to acquire invasive properties and to develop metastatic growth characteristics (16). Therefore, the present study hypothesized that DEPDC1B may be involved in the EMT process. To investigate this effect, the expression of EMT markers and EMT-inducing transcription factors (EMT-TFs) was analyzed in the present study. Western blotting assays revealed that the expression of the epithelial marker E-cadherin was increased, whereas the mesenchymal markers Vimentin and N-cadherin, and the EMT-TF Snail were markedly decreased in DEPDC1B

knockdown cells (Fig. 5). Conversely, downregulation of E-cadherin and upregulation of Vimentin, N-cadherin and Snail were detected in the cell lines overexpressing DEPDC1B (Fig. 5). There was no significant difference in the expression of Slug and Twist between the NC and treatment group. In addition, immunofluorescent staining was performed to analyze the protein expression of E-cadherin, Vimentin and N-cadherin. The results of the immunofluorescence assay further verified the alteration of EMT makers in DEPDC1B knockdown and overexpression cells (Fig. 6). These results indicated that DEPDC1B may be involved in the EMT process in PDAC cells.
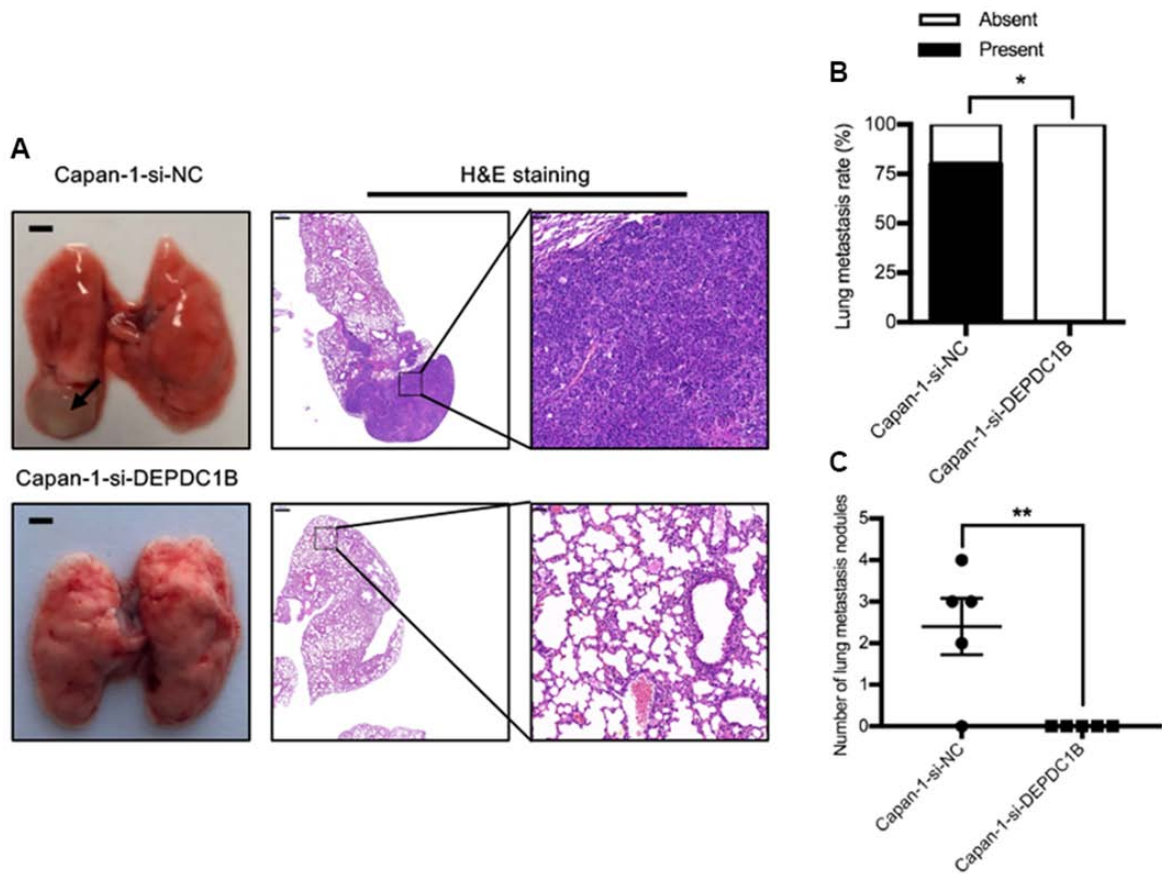
Figure 4. Effects of DEPDC1B on tumor metastasis *in vivo*. (A) Representative images of nude mice lung with or without metastasis. Scale bar, 2 mm. Hematoxylin and eosin staining of nude mice lung after injection of DEPDC1B knockdown and NC Capan-1 cells. Scale bars, 500 μm (left), 50 μm (right). (B) Incidence of lung metastasis (n=5). (C) Number of metastasis nodules in the lungs. *P<0.05; **P<0.01. NC, negative control; si, small interfering RNA; DEPDC1B, DEP domain containing 1B.
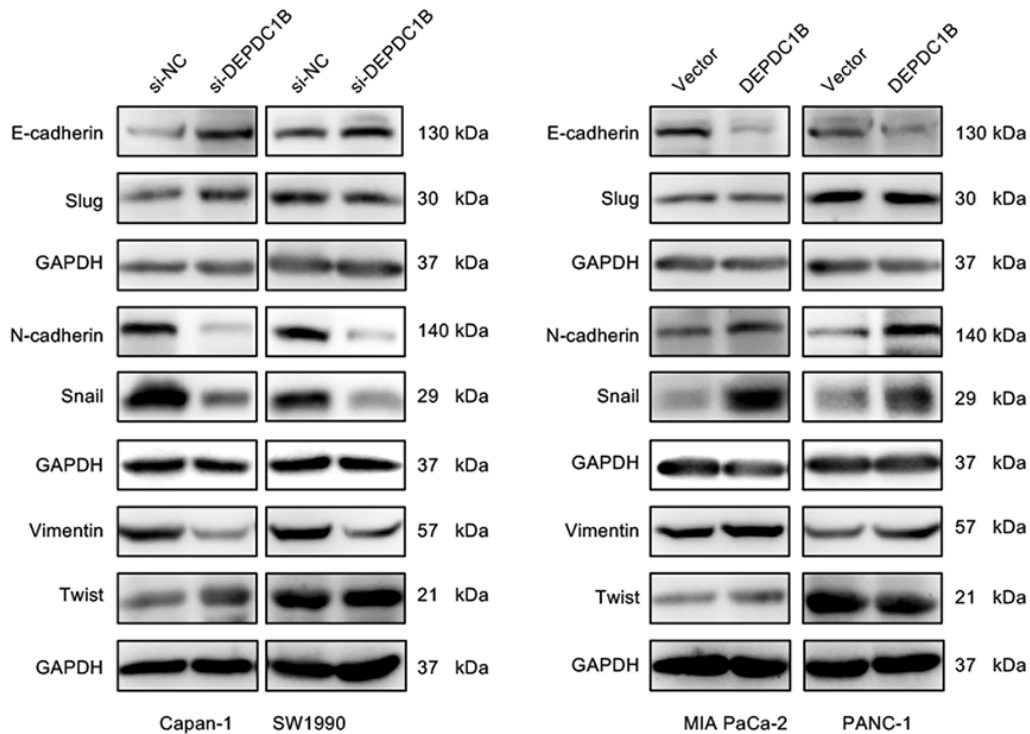

Figure 5. DEPDC1B induces EMT in pancreatic ductal adenocarcinoma cells. The protein expression levels of EMT markers (E-cadherin, N-cadherin and Vimentin) and EMT-inducing transcription factors (Snail, Slug and Twist) were measured by western blotting. GAPDH was used as the loading control. NC, negative control; si, small interfering RNA; DEPDC1B, DEP domain containing 1B; EMT, epithelial-mesenchymal transition.
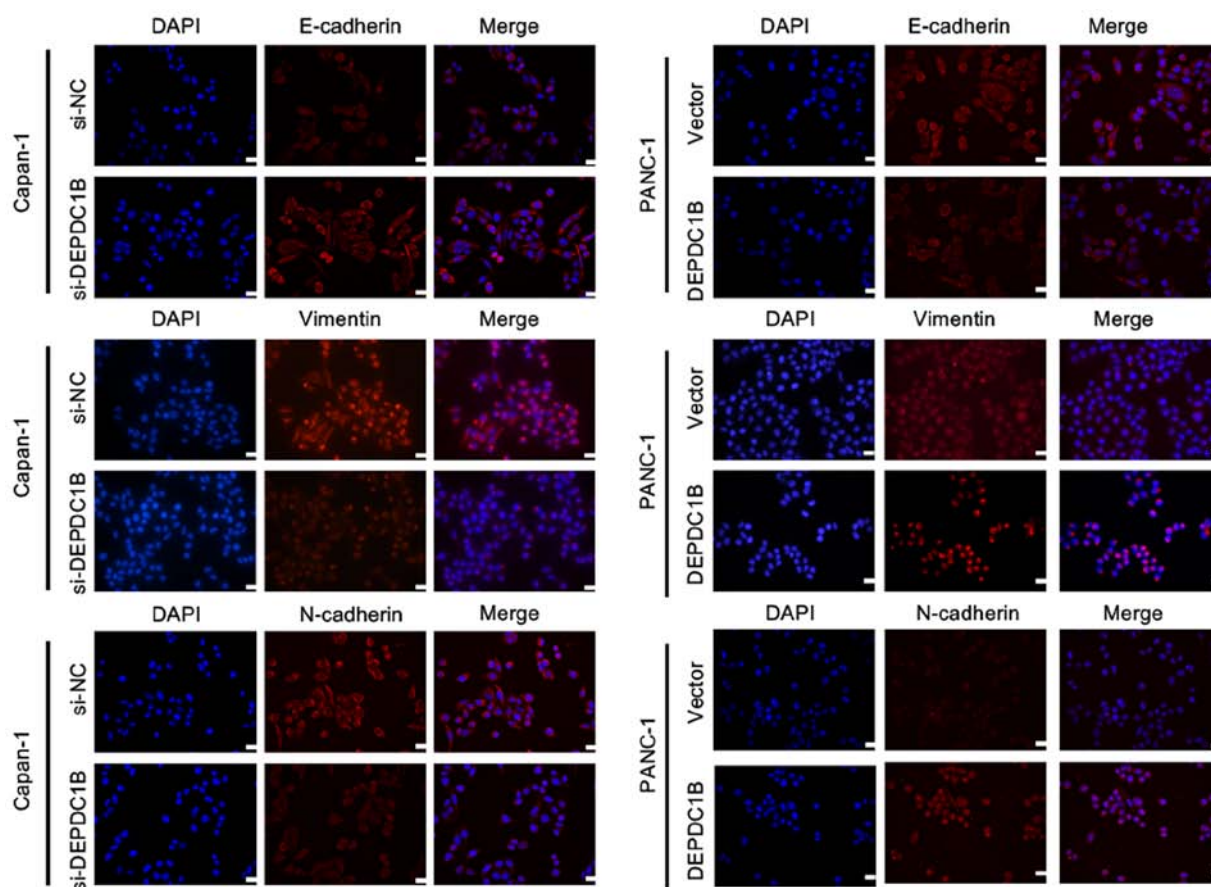
Figure 6. DEPDC1B induces epithelial-to-mesenchymal transition in pancreatic ductal adenocarcinoma cells. Representative immunofluorescent staining images of E-cadherin, Vimentin and N-cadherin expression in Capan-1 and PANC-1 cells. Scale bar, 20 μm. NC, negative control; si, small interfering RNA; DEPDC1B, DEP domain containing 1B.

DEPDC1B modulates the Akt/GSK3β/Snail signaling pathway in PDAC cells. As the main member of EMT-TFs, Snail can bind to the E-box area of E-cadherin and suppress its expression, thereby inducing EMT (32-34). Numerous studies have revealed that Akt can inhibit GSK3β activation and subsequently lead to the stabilization of endogenous Snail (24,25,35). The present study hypothesized that DEPDC1B may induce EMT via the Akt/GSK3β/Snail pathway. As presented in Fig. 7A, DEPDC1B overexpression significantly increased the levels of p-Akt at S473, p-GSK3β and Snail, whereas these protein levels were decreased in DEPDC1B knockdown cells. These findings suggested that DEPDC1B may enhance Snail expression via the Akt/GSK3β pathway. To further verify whether Snail upregulation was mediated by Akt, DEPDC1B overexpressing cells were treated with the Akt inhibitor LY294002. The results showed that LY294002 treatment reversed the upregulation of p-Akt, p-GSK3β and Snail induced by the overexpression of DEPDC1B in both PANC-1 and MIA PaCa-2 cells (Fig. 7B). In addition, the inhibition of Akt increased the protein expression levels of E-cadherin and decreased Vimentin and N-cadherin expression (Fig. 7B). These results suggested that DEPDC1B promoted EMT via the Akt/GSK3β/Snail signaling pathway.

Discussion

PDAC remains to be one of the most devastating diseases, and metastasis is a major challenge in clinical treatment.

Conventional treatments including surgery, chemotherapy and radiation have little effect on the course of the disease (36). In addition, clinical trials of various biological agents targeting specific signaling pathways or transcription factors have proved disappointing (37). For example, a randomized, double-blind, placebo-controlled trial (NCT01231581) of gemcitabine plus trametinib (an oral MEK inhibitor) did not improve OS, PFS, ORR or DOR in chemotherapy-naive patients with metastatic PDAC (38). Therefore, a deeper understanding of the molecular mechanisms underlying PDAC and finding new molecules to establish novel therapeutic targets remain an urgent requirement. Previous research investigating DEPDC1B has demonstrated its upregulation in several types of cancer (7-11). These studies have shown that DEPDC1B promotes the development of oral cancer via Rac-ERK1/2 pathway and enhances migration and invasion of NSCLC through Wnt/β-catenin signaling.

In the present study, the expression of DEPDC1B was found to be significantly increased in PDAC tissues compared with adjacent non-cancerous tissues. Furthermore, clinical data showed that upregulation of DEPDC1B is associated with poor prognosis of patients with PDAC. These results indicated that DEPDC1B may be involved in PDAC progression. In addition, the present study confirmed the important role of DEPDC1B in promoting PDAC migration and invasion. Likewise, DEPDC1B overexpression was found to induce EMT process and increase the expression of Snail.
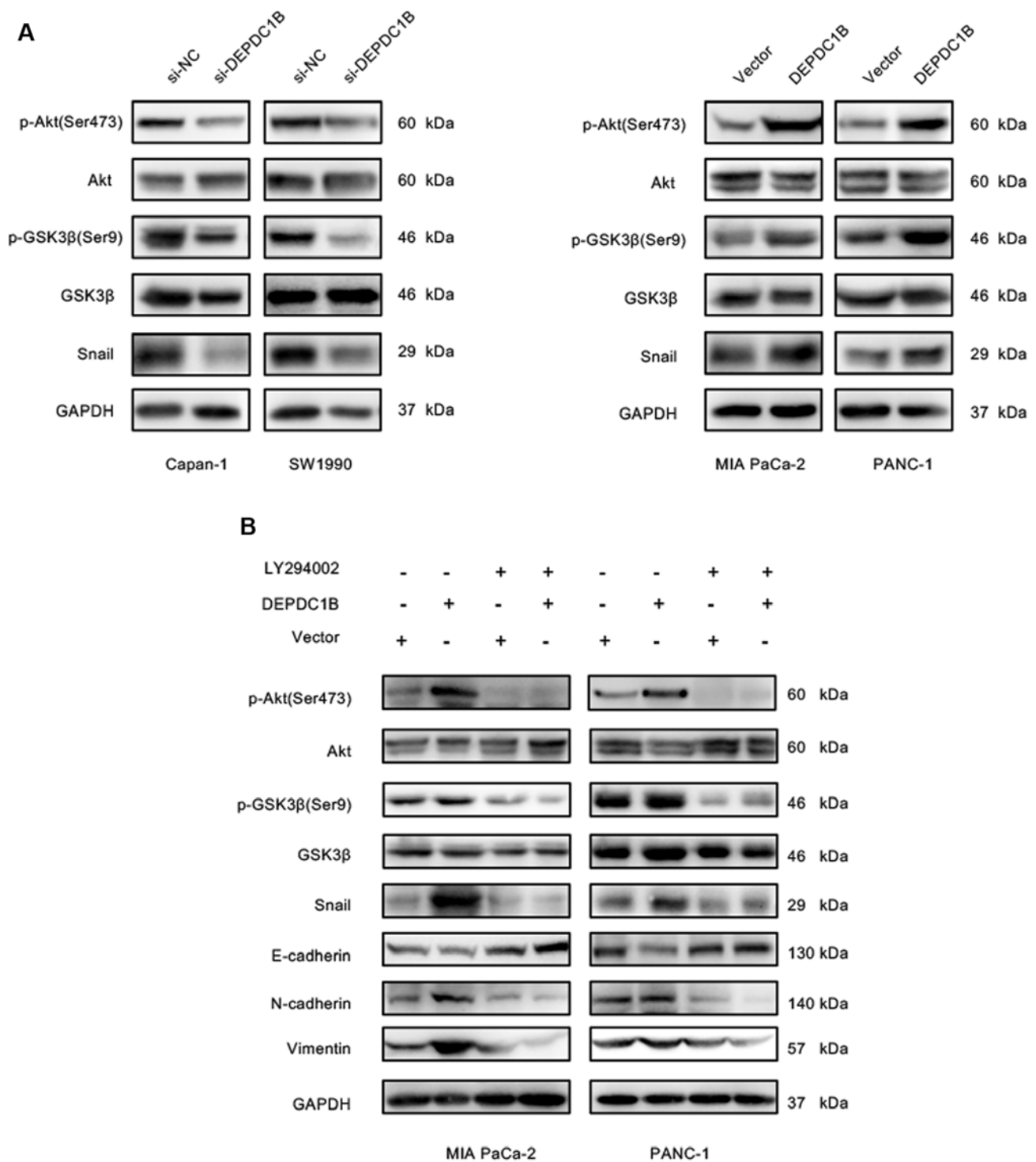
Figure 7. DEPDC1B induces EMT by activating the Akt/GSK3β/Snail signaling pathway. (A) Western blotting showed the expression of key proteins in the Akt/GSK3β/Snail signaling pathway. (B) Western blotting of Akt/GSK3β/Snail signaling and EMT markers in DEPDC1B overexpressing cells pretreated with or without LY294002 (50 μM). GAPDH was used as the loading control. NC, negative control; si, small interfering RNA; p-, phosphorylated; ETM, epithelial-to-mesenchymal transition.

Further analysis of metastasis-associated pathways revealed that p-Akt and p-GSK3β were involved in the observed effects driven by DEPDC1B on PDAC cells. Previous studies have revealed that the Akt/GSK3β/Snail signaling pathway regulates EMT (21-23), and in the present study, western blot results showed that overexpression of DEPDC1B enhanced the expression of p-Akt, p-GSK3β and Snail. In contrast, decreased expression of p-Akt, p-GSK3β and Snail was observed when

DEPDC1B was knocked down. In addition, treatment with the Akt inhibitor LY294002 decreased the expression of p-Akt, p-GSK3β and Snail, which subsequently affected E-cadherin, Vimentin and N-cadherin expression. Taken together, these findings indicate that DEPDC1B may mediate EMT through the Akt/GSK3β/Snail signaling pathway.

The present study reported the role of DEPDC1B in PDAC and the association between DEPDC1B and the

Akt/GSK3β/Snail pathway. The detailed interaction between DEPDC1B and Akt pathway may be attributed to the DEP domain that can regulate G protein-coupled receptor (GPCR)-initiated pathways via docking onto GPCRs (39,40), which can consequently activate the PI3K/Akt pathway (41-43). Therefore, further investigation on whether DEPDC1B activates the Akt pathway through the interaction between its DEP domain and GPCRs would be helpful to improve the current understanding of the mechanism underlying PDAC metastasis. In addition, there are a number of limitations to the present study, such as the lack of healthy controls and the lack of experiments performed on the same cell line.

In summary, the current study demonstrated that DEPDC1B is upregulated in PDAC tissues and cell lines, and it may work as a prognosis predictive marker for patients with PDAC. Furthermore, DEPDC1B promotes tumor migration and invasion and induces EMT via the regulation of Akt/GSK3β/Snail signaling pathway, which may represent a new therapeutic target for PDAC.

Acknowledgements

Not applicable.

Funding

Availability of data and materials

The datasets used and/or analyzed during the present study are available from the corresponding author on reasonable request.

Authors' contributions

XL, TL, QW and LFW conceived and designed the study. XL wrote the manuscript. XL and TL performed the majority of the experiments. XH and HX assisted with the collection of clinical samples and data. WW, JL, YQ and LW analyzed the experimental data. QW and LFW reviewed the manuscript. All authors read and approved the final manuscript.

Ethics approval and consent to participate

The present study was approved by the Ethics Committee of Ruijin Hospital. Written informed content was obtained from all patients. All animal experiments were approved by the institutional animal care and use committee of Shanghai Jiaotong University School of Medicine (IACUC approval no. B-2019-004).

Patient consent for publication

Not applicable.

Competing interests

The authors declare that they have no competing interests.

References

1. Siegel RL, Miller KD and Jemal A: Cancer statistics, 2018. CA Cancer J Clin 68: 7-30, 2018.
2. Kamisawa T, Wood LD, Itoi T and Takaori K: Pancreatic cancer. Lancet 388: 73-85, 2016.
3. Chen W, Zheng R, Baade PD, Zhang S, Zeng H, Bray F, Jemal A, Yu XQ and He J: Cancer statistics in China, 2015. CA Cancer J Clin 66: 115-132, 2016.
4. Marchesi S, Montani F, Deflorian G, D'Antuono R, Cuomo A, Bologna S, Mazzoccoli C, Bonaldi T, Di Fiore PP and Nicassio F: DEPDC1B coordinates de-adhesion events and cell-cycle progression at mitosis. Dev Cell 31: 420-433, 2014.
5. Garcia-Mata R: Arrested detachment: A DEPDC1B-mediated de-adhesion mitotic checkpoint. Dev Cell 31: 387-389, 2014.
6. Ahuja P and Singh K: In silico approach for SAR analysis of the predicted model of DEPDC1B: A novel target for oral cancer. Adv Bioinformatics 2016: 3136024, 2016.
7. Boudreau HE, Broustas CG, Gokhale PC, Kumar D, Mewani RR, Rone JD, Haddad BR and Kasid U: Expression of BRCC3, a novel cell cycle regulated molecule, is associated with increased phospho-ERK and cell proliferation. Int J Mol Med 19: 29-39, 2007.
8. Yang Y, Liu L, Cai J, Wu J, Guan H, Zhu X, Yuan J and Li M: DEPDC1B enhances migration and invasion of non-small cell lung cancer cells via activating Wnt/β-catenin signaling. Biochem Biophys Res Commun 450: 899-905, 2014.
9. Bai S, Chen T, Du T, Chen X, Lai Y, Ma X, Wu W, Lin C, Liu L and Huang H: High levels of DEPDC1B predict shorter biochemical recurrence-free survival of patients with prostate cancer. Oncol Lett 14: 6801-6808, 2017.
10. Su YF, Liang CY, Huang CY, Peng CY, Chen CC, Lin MC, Lin RK, Lin WW, Chou MY, Liao PH and Yang JJ: A putative novel protein, DEPDC1B, is overexpressed in oral cancer patients, and enhanced anchorage-independent growth in oral cancer cells that is mediated by Rac1 and ERK. J Biomed Sci 21: 67, 2014.
11. Xu Y, Sun W, Zheng B, Liu X, Luo Z, Kong Y, Xu M and Chen Y: DEPDC1B knockdown inhibits the development of malignant melanoma through suppressing cell proliferation and inducing cell apoptosis. Exp Cell Res 379: 48-54, 2019.
12. Valastyan S and Weinberg Robert A: Tumor metastasis: Molecular insights and evolving paradigms. Cell 147: 275-292, 2011.
13. Thiery JP, Acloque H, Huang RY and Nieto MA: Epithelial-mesenchymal transitions in development and disease. Cell 139: 871-890, 2009.
14. Chaffer CL, San Juan BP, Lim E and Weinberg RA: EMT, cell plasticity and metastasis. Cancer Metastasis Rev 35: 645-654, 2016.
15. Nieto MA, Huang RY, Jackson RA and Thiery JP: EMT: 2016. Cell 166: 21-45, 2016.
16. Rhim AD, Mirek ET, Aiello NM, Maitra A, Bailey JM, McAllister F, Reichert M, Beatty GL, Rustgi AK, Vonderheide RH, et al: EMT and dissemination precede pancreatic tumor formation. Cell 148: 349-361, 2012.
17. Hanahan D and Weinberg RA: Hallmarks of cancer: The next generation. Cell 144: 646-674, 2011.
18. Chen T, You Y, Jiang H and Wang ZZ: Epithelial-mesenchymal transition (EMT): A biological process in the development, stem cell differentiation, and tumorigenesis. J Cell Physiol 232: 3261-3272, 2017.
19. Rhim AD, Mirek ET, Aiello NM, Maitra A, Bailey JM, McAllister F, Reichert M, Beatty GL, Rustgi AK, Vonderheide RH, et al: EMT and dissemination precede pancreatic tumor formation. Cell 148: 349-361, 2012.
20. Mihaljevic AL, Michalski CW, Friess H and Kleeff J: Molecular mechanism of pancreatic cancer-understanding proliferation, invasion, and metastasis. Langenbecks Arch Surg 395: 295-308, 2010.
21. Lan Y, Han J, Wang Y, Wang J, Yang G, Li K, Song R, Zheng T, Liang Y, Pan S, et al: STK17B promotes carcinogenesis and metastasis via AKT/GSK-3β/Snail signaling in hepatocellular carcinoma. Cell Death Dis 9: 236, 2018.
22. Liu L, Dai Y, Chen J, Zeng T, Li Y, Chen L, Zhu YH, Li J, Li Y, Ma S, et al: Maelstrom promotes hepatocellular carcinoma metastasis by inducing epithelial-mesenchymal transition by way of Akt/GSK-3β/Snail signaling. Hepatology 59: 531-543, 2014.
23. Jiang H, Zhou Z, Jin S, Xu K, Zhang H, Xu J, Sun Q, Wang J and Xu J: PRMT9 promotes hepatocellular carcinoma invasion and metastasis via activating PI3K/Akt/GSK-3β/Snail signaling. Cancer Sci 109: 1414-1427, 2018.

24. Zhou BP, Deng J, Xia W, Xu J, Li YM, Gunduz M and Hung MC: Dual regulation of Snail by GSK-3beta-mediated phosphorylation in control of epithelial-mesenchymal transition. Nat Cell Biol 6: 931-940, 2004.
25. Bachelder RE, Yoon SO, Franci C, de Herreros AG and Mercurio AM: Glycogen synthase kinase-3 is an endogenous inhibitor of Snail transcription: Implications for the epithelial-mesenchymal transition. J Cell Biol 168: 29-33, 2005.
26. Zhou BP and Hung MC: Wnt, hedgehog, and snail: Sister pathways that control by GSK-3beta and beta-Trcp in the regulation of metastasis. Cell Cycle 4: 772-776, 2005.
27. Badea L, Herlea V, Dima SO, Dumitrascu T and Popescu I: Combined gene expression analysis of whole-tissue and microdissected pancreatic ductal adenocarcinoma identifies genes specifically overexpressed in tumor epithelia. Hepatogastroenterology 55: 2016-2027, 2008.
28. Pei H, Li L, Fridley BL, Jenkins GD, Kalari KR, Lingle W, Petersen G, Lou Z and Wang L: FKBP51 affects cancer cell response to chemotherapy by negatively regulating Akt. Cancer Cell 16: 259-266, 2009.
29. Donahue TR, Tran LM, Hill R, Li Y, Kovochich A, Calvopina JH, Patel SG, Wu N, Hindoyan A, Farrell JJ, *et al*: Integrative survival-based molecular profiling of human pancreatic cancer. Clin Cancer Res 18: 1352-1363, 2012.
30. Shen R, Wang Q, Cheng S, Liu T, Jiang H, Zhu J, Wu Y and Wang L: The biological features of PanIN initiated from oncogenic Kras mutation in genetically engineered mouse models. Cancer Lett 339: 135-143, 2013.
31. Livak KJ and Schmittgen TD: Analysis of relative gene expression data using real-time quantitative PCR and the 2(-Delta Delta C(T)) method. Methods 25: 402-408, 2001.
32. Xu W, Yang Z and Lu N: A new role for the PI3K/Akt signaling pathway in the epithelial-mesenchymal transition. Cell Adh Migr 9: 317-324, 2015.
33. Wang Y, Shi J, Chai K, Ying X and Zhou BP: The role of snail in EMT and tumorigenesis. Curr Cancer Drug Targets 13: 963-972, 2013.
34. Nieto MA: The snail superfamily of zinc-finger transcription factors. Nat Rev Mol Cell Biol 3: 155-166, 2002.
35. Qiao M, Sheng S and Pardee AB: Metastasis and AKT activation. Cell Cycle 7: 2991-2996, 2014.
36. Ryan DP, Hong TS and Bardeesy N: Pancreatic adenocarcinoma. N Engl J Med 371: 2140-2141, 2014.
37. Garrido-Laguna I and Hidalgo M: Pancreatic cancer: From state-of-the-art treatments to promising novel therapies. Nat Rev Clin Oncol 12: 319-334, 2015.
38. Infante JR, Somer BG, Park JO, Li CP, Scheulen ME, Kasubhai SM, Oh DY, Liu Y, Redhu S, Steplewski K and Le N: A randomised, double-blind, placebo-controlled trial of trametinib, an oral MEK inhibitor, in combination with gemcitabine for patients with untreated metastatic adenocarcinoma of the pancreas. Eur J Cancer 50: 2072-2081, 2014.
39. Ballon DR, Flanary PL, Gladue DP, Konopka JB, Dohlman HG and Thorner J: DEP-domain-mediated regulation of GPCR signaling responses. Cell 126: 1079-1093, 2006.
40. Consonni SV, Maurice MM and Bos JL: DEP domains: Structurally similar but functionally different. Nat Rev Mol Cell Biol 15: 357-362, 2014.
41. Khalil BD, Hsueh C, Cao Y, Abi Saab WF, Wang Y, Condeelis JS, Bresnick AR and Backer JM: GPCR signaling mediates tumor metastasis via PI3Kβ. Cancer Res 76: 2944-2953, 2016.
42. Murga C, Fukuhara S and Gutkind JS: A novel role for phosphatidylinositol 3-kinase beta in signaling from G protein-coupled receptors to Akt. J Biol Chem 275: 12069-12073, 2000.
43. Dbouk HA, Vadas O, Shymanets A, Burke JE, Salamon RS, Khalil BD, Barrett MO, Waldo GL, Surve C, Hsueh C, *et al*: G protein-coupled receptor-mediated activation of p110beta by Gbetagamma is required for cellular transformation and invasiveness. Sci Signal 5: ra89, 2012.
44. Allen PJ, Kuk D, Castillo CF, Basturk O, Wolfgang CL, Cameron JL, Lillemoe KD, Ferrone CR, Morales-Oyarvide V, He J, *et al*: Multi-institutional validation study of the American joint commission on cancer (8th Edition) changes for T and N staging in patients with pancreatic adenocarcinoma. Ann Surg 265: 185-191, 2017.